Capacitive beam position monitors for the low-β beam of the Chinese ADS proton linac*

Yong Zhang(张雍)[1;1)] Jun-Xia Wu(武军霞)[1] Guang-Yu Zhu(朱光宇)[1,2] Huan Jia(贾欢)[1,2]
Zong-Heng Xue(薛纵横)[1] Hai Zheng(郑海)[1] Hong-Ming Xie(谢宏明)[1,3] Xin-Cai Kang(康新才)[1]
Yuan He(何源)[1] Lin Li(李林)[4,5] Jean Claude Denard [6]

[1] Institute of Modern Physics, Chinese Academy of Sciences, Lanzhou 730000, China
[2] University of Chinese Academy of Sciences, Beijing 100049, China
[3] University of Science and Technology of China, Hefei 230022, China
[4] Institute of Microelectronics, School of Physical Science and Technology, Lanzhou University, Lanzhou 730000, China
[5] Lanzhou Institute of Physics, Chinese Academy of Space Technology, Lanzhou 730000, China
[6] Consultant and Synchrotron SOLEIL, Saint-Aubin, France

Abstract: Beam Position Monitors (BPMs) for the low-β beam of the Chinese Accelerator Driven Subcritical system (CADS) Proton linac are of the capacitive pick-up type. They provide higher output signals than that of the inductive type. This paper will describe the design and tests of the capacitive BPM system for the low-β proton linac, including the pick-ups, the test bench and the read-out electronics. The tests done with an actual proton beam show a good agreement between the measurements and the simulations in the time domain.

Keywords: beam position monitor, low-β beam, capacitance, coupling strength, linear accelerator

PACS: 29.20.Ej **DOI:** 10.1088/1674-1137/40/2/027003

1 Introduction

The Chinese Accelerator-Driven Subcritical system (CADS) is part of a strategic plan aimed at solving the nuclear waste problem in China. This project is based on a Continuous Wave (CW) proton linac that produces a 10 mA current of high energy protons at 1.5 GeV, directed towards a spallation target and causing a subcritical reaction between the nuclear waste and the neutrons. In the initial stage, there will be two injector linacs to supply proton beams; this is to get the high reliability needed for this kind of project. Injector I, built by the Institute of High Energy Physics (IHEP) in Beijing, is producing a 10 mA CW proton beam at 10 MeV, with an RF frequency of 325 MHz. The Institute of Modern Physics (IMP) in Lanzhou is building the Injector II linac; it will supply the same energy proton beam but with an RF frequency of 162.5 MHz. It consists of an Electron Cyclotron Resonance (ECR) ion source, a Low Energy Beam Transport (LEBT) line at 35 keV, a Radio Frequency Quadrupole accelerator (RFQ), a Medium Energy Beam Transport (MEBT) line at 2.1 MeV, and two cryomodules to bring the proton energy up to 10 MeV [1].

Non-interceptive Beam Position Monitors (BPMs) will be installed into the MEBT and the cryomodules in order to measure the transverse beam position and the beam phase. For many proton linac facilities, the BPMs are usually of the stripline type for short bunch observation. They can be installed inside a quadruple magnet in order to save space in the longitudinal direction. The inductive BPM signal has been evaluated and compared to the capacitive pick-up type. There are many excellent review articles on the analysis of stripline BPMs (see, for example, [2–8]).

However, when a slow beam goes through a BPM, the longitudinal distribution of the wall current in the vacuum tube is lengthened. The wall current lengthening reduces the high-frequency Fourier components of the beam current induced in the pick-up electrodes, which results in lower output signal power. It also modifies the BPM sensitivity to beam displacement [9, 10]. Therefore improving the output signal power and getting a high transfer sensitivity of the BPMs has been the most important consideration when designing the BPMs for the low-β proton linac. This paper shows that using numerical analysis and beam tests, the capacitive pick-up electrodes are more efficient, in terms of output signal

Received 30 April 2015
* Supported by National Natural Science Foundation of China (11405240) and "Western Light" Talents Training Program of Chinese Academy of Sciences
1) E-mail: zhangy@impcas.ac.cn

power, than inductive ones like stripline BPMs. Then, the new capacitive BPM system for the low-β beam of the CADS Injector II proton linac, including two kinds of pick-up for the MEBT and the cryomodule, test bench and read-out electronics has been designed, built and tested on a real proton beam.

2 Capacitive BPMs

2.1 Comparison between inductive and capacitive BPMs

In general, the output signal in the time domain for a capacitive BPM (as shown in Fig. 1(a)) is given by:

$$i(t)=\frac{\mathrm{d}Q}{\mathrm{d}t}=\frac{\mathrm{d}}{\mathrm{d}t}\int \boldsymbol{D}\cdot\mathrm{d}\boldsymbol{s}=\frac{\mathrm{d}}{\mathrm{d}t}\int \varepsilon_0 E_\mathrm{r}\mathrm{d}\boldsymbol{s}, \tag{1}$$

where E_r is the radial component of the electric field associated with the moving charged particles, and $\epsilon_0 = 8.85\times10^{-12}$ F/m is the vacuum permittivity. For a stripline electrode (as shown in Fig. 1(b)), the magnetic flux variation in the loop induces a signal $u(t)$ on the electrode output:

$$u(t)=-\frac{\mathrm{d}}{\mathrm{d}t}\int \boldsymbol{B}\mathrm{d}\boldsymbol{s}=-\frac{\mathrm{d}}{\mathrm{d}t}\int B_\Phi\mathrm{d}\boldsymbol{s}, \tag{2}$$

where B_Φ is the azimuthal component of the magnetic field.

According to the well-known relation $\boldsymbol{B}=\dfrac{\boldsymbol{v}}{c^2}\times\boldsymbol{E}\Rightarrow B_\Phi=\beta/cE_\mathrm{r}$ [11], the ratio between capacitive and inductive signals on the electrode outputs can be estimated as a function of the β value:

$$\begin{aligned}\left|\frac{i(t)}{u(t)}\right|&=\left|\frac{\dfrac{\mathrm{d}}{\mathrm{d}t}\displaystyle\int\epsilon_0\boldsymbol{E}_\mathrm{r}\mathrm{d}\boldsymbol{s}}{-\dfrac{\mathrm{d}}{\mathrm{d}t}\displaystyle\int B_\Phi\mathrm{d}\boldsymbol{s}}\right|\\&=\frac{c\epsilon_0}{\beta}\frac{\dfrac{\mathrm{d}}{\mathrm{d}t}\displaystyle\int_{\text{capacitive coupling plate}}\boldsymbol{E}_\mathrm{r}\mathrm{d}\boldsymbol{s}}{\dfrac{\mathrm{d}}{\mathrm{d}t}\displaystyle\int_{\text{inductive coupling loop}}\boldsymbol{E}_\mathrm{r}\mathrm{d}\boldsymbol{s}}.\end{aligned} \tag{3}$$

In our case, the ratio of both integral terms in Eq. (3) is very close to one with an identical size of the two pick-ups. Taking this into account and assuming broadband signal processing with an impedance of $R = 50\ \Omega$, we get:

$$\left|\frac{u_\text{capacitive}}{u_\text{inductive}}\right|=\left|\frac{i(t)R}{u(t)}\right|\approx\frac{c\epsilon_0R}{\beta}\approx\frac{0.133}{\beta}. \tag{4}$$

Thus, with equivalent electrode areas, the output signal from a capacitive electrode is higher for low β (< 0.133) beams than that of an inductive one.

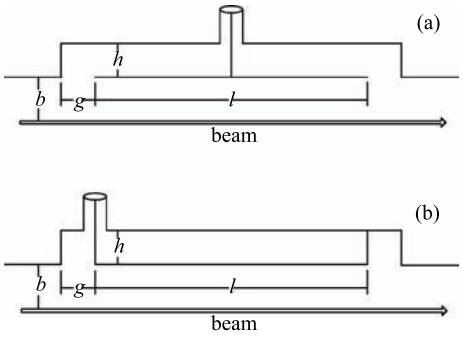

Fig. 1. Schematic view of a capacitive BPM electrode (a) and of an inductive one (b) (shorted stripline)

The numerical simulations for low β beams were performed with CST Particle Studio (CST PS) using the wake-field solver [12, 13]. As a source of excitation a pencil beam at $\beta = 0.073$ was entered with a Gaussian-shaped longitudinal charge distribution. The bunch length was $\sigma = 230$ ps (about 5 mm) and the bunch frequency was 162.5 MHz. As shown in Fig. 2, the output signal of capacitive electrodes is significantly higher than that of striplines. We are mainly concerned

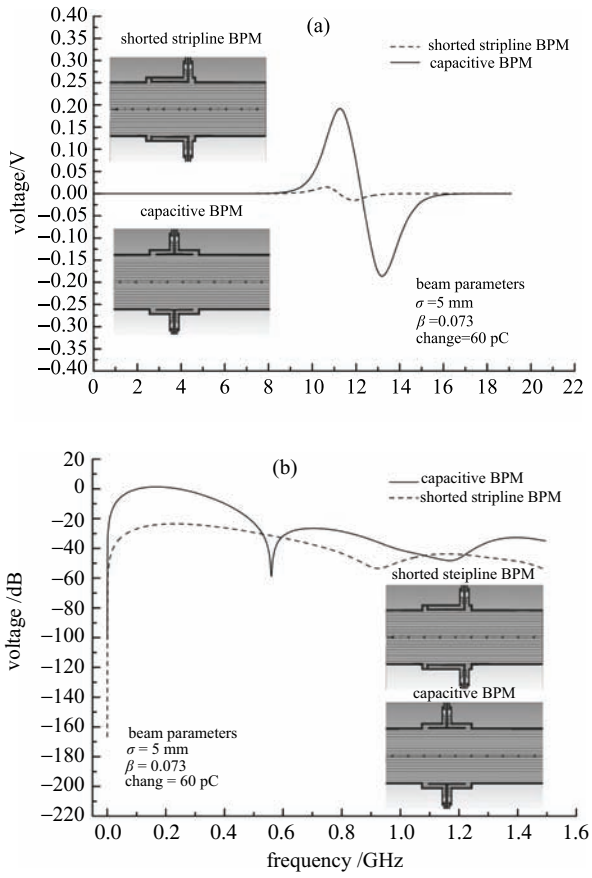

Fig. 2. Comparison between output signals from two different kinds of BPM electrode of the same size, (a) in the time domain, and (b) in the frequency domain.

with the magnitude of the pick-up signals at 162.5 MHz and 325 MHz, the fundamental and first harmonic frequencies, thus the capacitive BPM is the best choice for our proton linac.

In 2013, we built a capacitive BPM and installed it in a proton linac at IHEP, as shown in Fig. 3(a). The IHEP proton linac can accelerate a pulsed proton beam of 15 mA up to an energy of 3.5 MeV with a Radio Frequency (RF) field at 352.2 MHz. Existing stripline BPMs, installed inside quadruple magnets, and our nearby capacitive BPM, are close to the beam dump at the end of the linac. Figure 3(b) shows the output signals of the two kinds of BPM. Channel 2 is connected to the inductive BPM (106 mm length and 45° angular width striplines [14]), and channel 1 is connected to the capacitive BPM (35 mm length and 42° angular width electrodes). Each of the BPMs is connected to the oscilloscope by a 50 m LMR cable. The capacitive BPM is located 1.16 m downstream from the inductive BPM. The drift space lengthens the bunches, which decreases its higher harmonics content. However, the capacitive BPM is still more efficient in terms of output signal power than the inductive one for a low-β beam at the interesting frequencies.

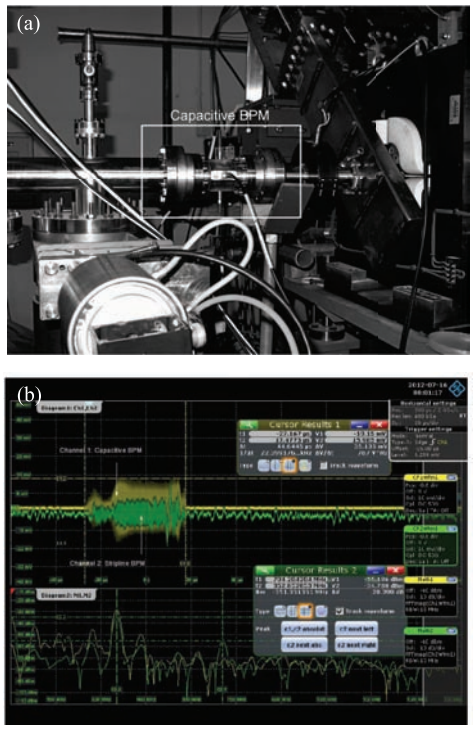

Fig. 3. (color online) (a) Photograph of the capacitive button BPM installed in the IHEP proton linac. (b) Comparison of the output signal envelopes of the stripline and capacitive BPMs in pulsed mode. During the macro-pulse duration of 50 μs, the 15 mA and 3.5 MeV beam is bunched by the RF at 352.2 MHz.

2.2 Capacitive pick-ups

Table 1 shows the beam properties and requirements for the BPMs of the CADS Injector II linac. In normal operation, the accelerator will work with CW beams but during its commissioning and tuning phases, the beam will be mostly pulsed at low duty factors. Therefore, the BPM design needs to address both operation modes. Considering the requirements and the space limitation on the transport line, we designed two different kinds of capacitive pick-ups, one for the MEBT and the other for the cryomodule. The detailed parameters of the BPMs have been optimized with CST Particle Studio.

Table 1. Beam properties for the CADS Injector II linac.

parameter	value
beam pipe diameter	50 / 40 mm
beam energy	2.1–10 MeV
bunch frequency	162.5 MHz
beam pulse length	0.1 ms - CW
bunch length $\sigma_{\rm rms}$	0.1–0.5 ns
average current	0.01–10 mA
peak current	20 mA
position accuracy	1% of half-aperture
position resolution	0.1% of half-aperture
phase accuracy	1–3 degree
phase resolution	0.1–0.3 degree
current accuracy	1% of full current

The monitor geometries and pictures are shown in Figs. 4(a) and (b) respectively. In the MEBT, the BPMs will be mounted inside the bore of the quadrupole magnets. It is made of stainless steel (AISI 304) with $\pi/2$ rotational symmetry. The total length is 150 mm. As previously shown in Fig. 1(a), the electrodes are 35 mm long with angular widths of 42°. The space h between electrode and core is of 2.5 mm in order to match the impedance to 50 Ω, and the space g is set to 5 mm, for the transit time factor. The four standard Kyocera 50 Ω feedthroughs are terminated by SMA connectors for space saving. The electrodes are recessed by 0.5 mm inside the beam pipe to prevent them from beam damage.

In the cryomodule, the cold BPMs are essential; they are the only diagnostics components between the Superconducting Half Wave Resonator (HWR) and the Superconducting solenoid. The materials for the cold button BPM have been investigated, and finally we decided to collaborate with Kyocera to build a button pick-up and feedthrough together. The detailed geometry is shown in Fig. 4(c). It consists of an N-connector feedthrough with a ϕ70 mm flange and a curved ϕ20.8 mm button. The gap between beam pipe and button along the longitudinal direction is 3.4 mm for the 50 Ω matching. The whole

BPM body, with a 150 mm length, is made of stainless steel (AISI 316LN) with a maximum magnetic permeability of 1.05 after the manufacturing process. These button BPMs have successfully passed the thermal test cycles between warm (300 K) to cold (4 K) temperatures. Precisely machined surfaces for alignment targets are shown and marked as Table 2 in Fig. 4(a) and label 4 in Fig. 4(c).

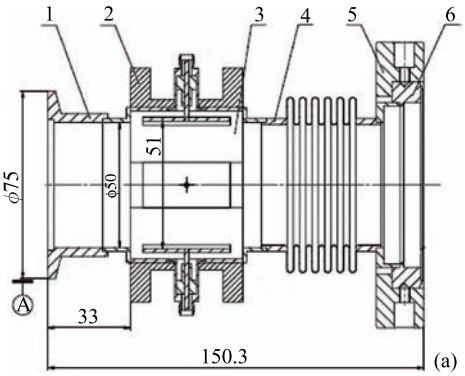

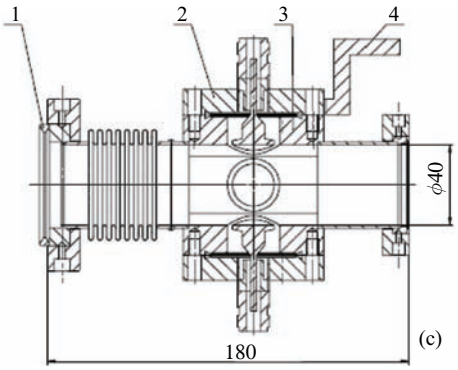

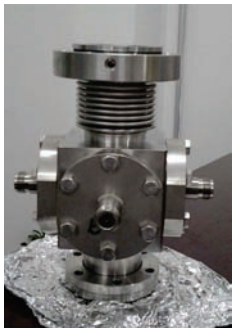

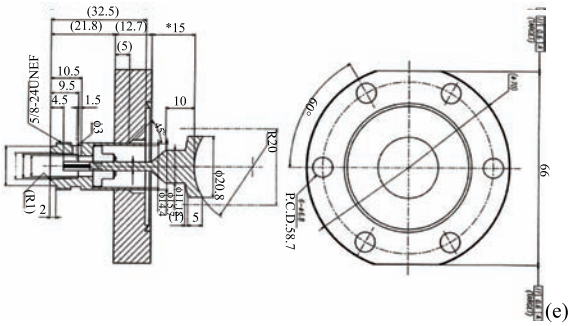

Fig. 4. Geometries and photographs of the capacitive BPMs: (a) and (b) for the MEBT, (c) and (d) for the cryomodules, and (e) drawing of a cold BPM button mounted on a flange with its feedthrough, made by Kyocera.

Table 2. Capacity measurements of BPM electrodes and error in the different ports.

BPM number	port 1/pF	port 2/pF	port 3/pF	port 4/pF	error
MEBT-BPM1	5.23	5.20	5.24	5.07	0.08
MEBT-BPM2	5.23	5.09	5.07	5.05	0.08
MEBT-BPM3	5.12	5.27	5.15	5.21	0.07
MEBT-BPM4	5.15	5.20	5.12	5.16	0.03
cryomodule button BPM	4.96	4.96	5.07	4.96	0.06

3 Measurements and tests

3.1 Measurements of the BPM characteristics

The capacitance measurements were performed with a Rohde Schwarz ZVA8 Vector Network Analyzer. We can get the electrode capacitances at low frequency in two ways, as shown in Fig. 5: by measuring the S11 Smith Chart parameter in the frequency domain from 2 MHz to 6.4 GHz with an IF width of 1 kHz and 3200 sweeping points, or by measuring the S11 real part using the low pass step mode in the time domain. It is known

that the capacitive BPM has a high-pass-like characteristic, with different behaviors on each side of the cutoff frequency $f_c = 1/(2\pi ZC)$[8, 9]. According to the measurements listed in Table 2, the average capacity of the electrodes including the feedthrough is about 5 pF. The capacity of the feedthrough itself is about 1.4 pF. The cutoff frequency of this capacitive BPM is about 885 MHz. The output voltage from capacitive BPMs depends on the capacity of the button electrode but also on the surface area. Thus a large electrode surface and a good uniformity of the four electrode capacities are important issues.

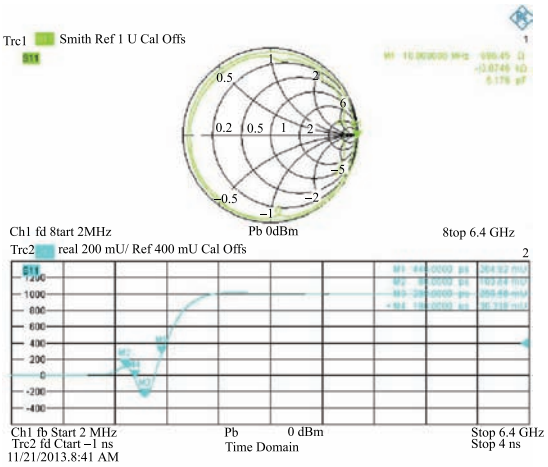

Fig. 5. (color online) Capacity measurement of BPM electrodes. The capacity of 5.176 pF is marked in trace 1 at 10 MHz, which is in agreement with the TDR result of 5.16 pF in trace 2. The capacity of the feedthrough itself is included.

3.2 Electromagnetic coupling between electrodes

Although a large angular width, resulting in a large electrode surface area, is desirable for a high signal-to-noise ratio, the coupling between adjacent electrodes is enhanced and affects the sensitivity of the BPM to the beam position. Thus, the coupling strength between electrodes must be taken into account in the design process. Using an RF network analyzer, the coupling strength between electrodes 1, 2, 3 and 4 were obtained by measuring the parameters S21, S31 and S41 in the frequency domain. The results are in agreement with the simulations, as shown in Fig. 6. The measured values are listed in Table 3.

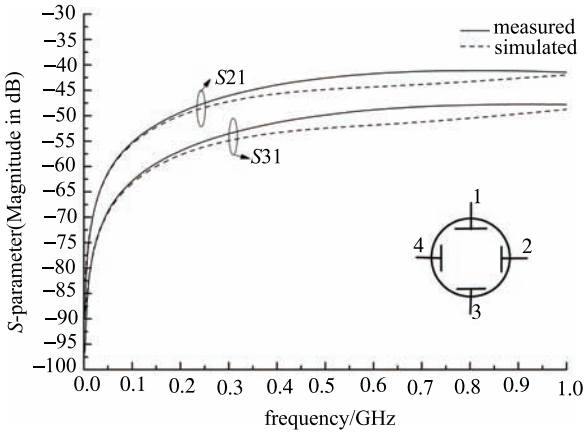

Fig. 6. Comparison between coupling measurements and simulations for the two different electrode configurations of a capacitive BPM (adjacent and opposite electrodes).

3.3 Test-bench calibration system

Figure 7 shows the test bench used for calibrating the BPMs. The 50 mm diameter BPM body is fixed on an X-Y-Z translation table and a wire of ϕ0.5 mm is stretched and fixed on the center along the Z direction. The stage can move in three dimensions by the step-motors along the X, Y and Z axes with a precision of 1 μm in the closed-loop control. Two resistances of 210 Ω are in series at each end of the wire in order to match the cable impedance. The calibration bench has measured the BPM electrical center to a precision better than 20 μm. An Agilent 81133A pulse generator drives the wire at a frequency of 162.5 MHz with the proper duty factors that simulate the pulsed beams. The electrode signals are connected, via 20 m cables (Times TCOM240) to a Libera Single Pass H from Instrumentation Technologies.

The Libera Single Pass H directly yields the beam transverse position and beam phase at the fundamental and the first harmonic frequency. It has analog signal processing functionality that selects the frequency

Table 3. Measured coupling strength between electrodes and errors in simulation and measurement at 162.5 MHz /325 MHz.

BPM number	$S21$/dB	$S31$/dB	$S41$/dB	$S21$ error	$S31$ error
MEBT-BPM1	−51.5/−45.5	−58.7/−52.9	−50.6/−44.9	1.7%/3.7%	2.4%/5.3%
MEBT-BPM2	−51.0/−45.3	−58.9/−53.1	−51.0/−45.4	1.9%/4.2%	2.0%/4.9%
MEBT-BPM3	−51.2/−45.6	−58.8/−53.0	−51.1/−45.5	1.5%/3.5%	2.2%/5.1%
MEBT-BPM4	−51.2/−45.6	−58.9/−53.1	−51.4/−45.8	1.5%/3.6%	2.0%/4.9%
cryomodule button BPM	−52.1/−45.3	−59.4/−54.5	−52.0/−46.0	1.9%/4.3%	2.4%/5.0%

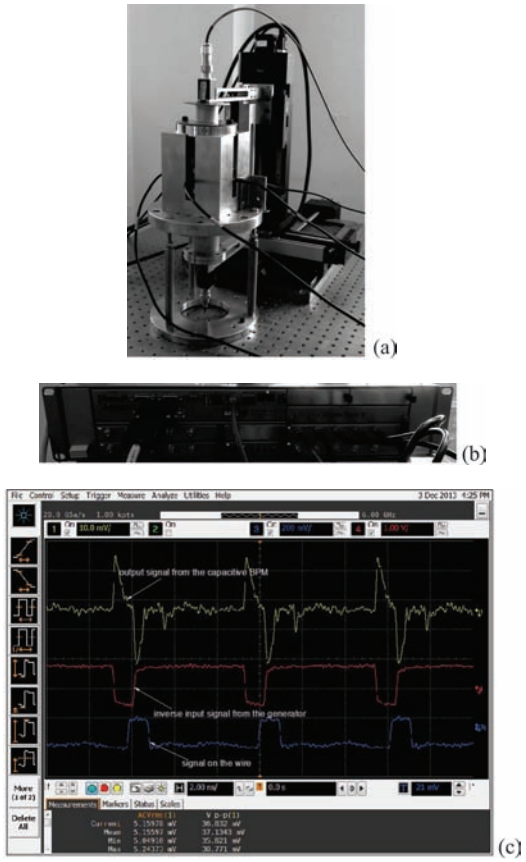

Fig. 7. (color online) The calibration system, including (a) the test bench with an Agilent 81133A Pulse generator, and (b) the Libera Single Pass H. (c) Agilent Infiniium Oscilloscope DSO90604A, which shows the output signals from the pick-up, the inverse input signal from the generator, and the signal on the wire. The signal frequency is 162.5 MHz.

components of interest and measures the signal amplitudes via the undersampling technique. Furthermore a reference Master Oscillator (MO) signal is digitized in parallel. The MO signal provides the stable frequency reference necessary for phase measurements [15].

Figure 8 shows the calibration results of a BPM with a Libera Single Pass H. As shown in Fig. 8(a), the radius of the linear area for this BPM is 2 mm around its center with a sensitivity factor S of 9.4 %/mm. This factor, once entered in the formula X (or Y) $= 1/S{\cdot}\Delta U/\Sigma U$, yields the beam position X (or Y). The amplitudes of the fundamental and first harmonic, respectively at 162.5 MHz and 325 MHz are measured with the spectrum analyzer without the read-out electronics while the BPM is installed on the calibration bench. Then, the coefficient factor K_x or K_y $(= 1/S)$ will be confirmed and will be input into the Libera Signal Pass H in order to perform the mapping. The mapping results are shown in Fig. 8(b).

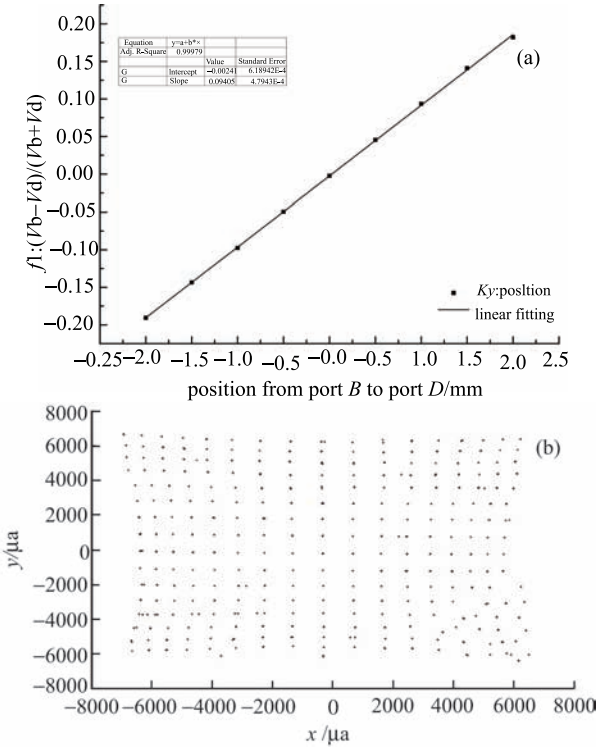

Fig. 8. (a) Difference over sum of two opposite electrodes versus the wire position with 1 mm displacement steps along the y-axis and (b) mapping with 1 mm displacement steps for the button type capacitive BPM at the fundamental frequency of 162.5 MHz with a Libera Single Pass H.

4 Beam test

A test RFQ linac of a few meters has been built at IMP. As shown in Fig. 9, it is equipped with several kinds of current transformer and one capacitive BPM. The linac can supply a pulsed or CW proton beam of 10 mA at 580 keV. The RF system accelerates and bunches the beam at 162.5 MHz. The output signal from the BPM is directly connected to the Agilent Infiniium Oscilloscope DSO90604A via four LMR cables of length 50 meters. As shown in Fig. 10, the output signals of the BPM in the time domain are in good agreement with the simulation.

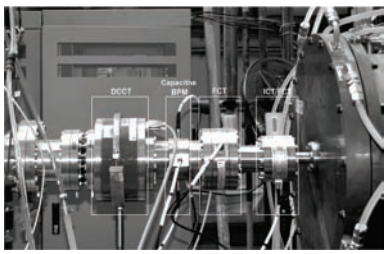

Fig. 9. The diagnostic components on the test RFQ linac.

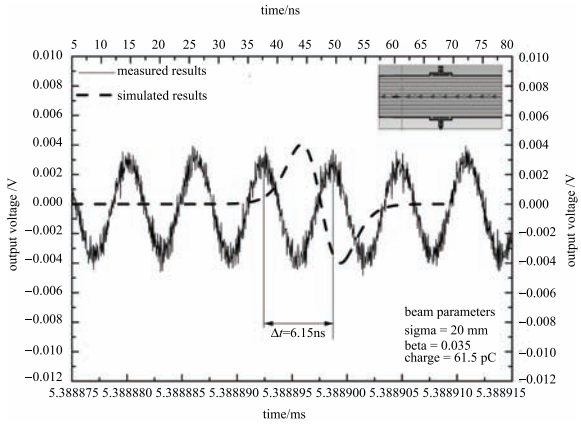

Fig. 10. Comparison of the BPM output signals with a CW beam at 162.5 MHz with the simulation done with a single bunch by CST PS. The beam energy is 580 keV with a current of 10 mA. The electrode length is 35 mm with angular widths of 45°. The beam pipe diameter is 90 mm.

5 Conclusions

Based on the comparison of the output signals' power between inductive and capacitive BPM, the CADS Injector II Proton Linac will be equipped with capacitive BPMs. The design, calibration and test of the prototype has been completed. CST simulations have been checked with a real beam. They will be the basis for defining the dynamic range needed for the Libera Single Pass H. The calibration system has been built and commissioned. Next steps will be i) measuring the RMS noise versus input power, ii) analyzing the error sources in the acquisition and the mechanical systems, and iii) calibrating all BPMs and installing them on the CADS Injector II linac.

The authors thank Prof. CAO Jianshe and Prof. XU Taoguang from IHEP for their efforts to install our capacitive BPM into the Proton LINAC in IHEP in Beijing. They also gratefully acknowledge Prof. Fritz Casper from CERN and Dr. Piotr Kowina from GSI for their help in measuring the small capacitances of the BPM and improving the performance of the calibration system.

References

1 Y. He, et al, in *Proceedings of IPAC* (Spain, 2011) p. 2613
2 R. E. Shafer, AIP Conf. Proc., **212**: 26 (1990)
3 S. R. Smith, AIP Conf. Proc., **390**: 50 (1997)
4 T. Suwada et al, Nucl. Instrum. Methods A, **440**: 307 (2000)
5 T. Suwada, Nucl. Instrum. Methods A, **705**: 7 (2013)
6 N. Hayashi et al, Nucl. Instrum. Methods A, **677**: 94 (2012)
7 M. Bai et al, Nucl. Instrum. Methods A, **499**: 372 (2003)
8 P. Forck et al, Beam Position Monitors, in *CERN Accelerator School on Beam Diagnostics*, (2008)
9 R. E. Shafer, in *Proc. Beam Instr. Workshop (BIW)*, (Santa Fe 1993) p.303
10 M. Cohen-Solal, Phys. Rev. Spec. TOP - AC, **13**: 032801 (2010)
11 P. Strehl, *Beam instrumentation and diagnostics* (Berlin: Springer, 2006) p.156
12 P. Kowina et al, in *Proceedings of DIPAC* (Basel, Switzerland, 2009) p.35
13 www.cst.com
14 Y. F. Ruan et al, Chinese Phys. C, **33**(3): 240–244 (2009)
15 User Manual, Libera Single Pass H, www. i-tech.si, (2013)